**8.4**

# Use of lightning data to enhance radar assimilation within the RUC and Rapid Refresh models

Stephen S. Weygandt[1], Stanley G. Benjamin[1], Ming Hu[1,2], Tatiana G. Smirnova[1,2], and John M. Brown[1]

[1]NOAA Earth System Research Laboratory, Global Systems Division, Boulder, CO, USA

[2]Cooperative Institute for Research in Environmental Sciences (CIRES), Boulder, CO, USA

## 1. Introduction

An ongoing research effort within NOAA ESRL/GSD has focused on incorporating lighting data into the RUC and Rapid Refresh analysis systems. For both systems, lightning data are converted to proxy radar reflectivity data using simple assumptions. Within the RUC, latent heating-based temperature tendency fields are then created, which are used to induce convective-scale circulations during a diabatic initialization step within the RUC model. Details of this are given below in sections 2-4. The technique is also being ported to the Gridpoint Statistical Interpolation (GSI) analysis package (developed by NCEP) that is being used for the Rapid Refresh.

We currently have access to NLDN data over CONUS and BLM lightning data over Alaska as indicated in Figs. iii, and i. The Alaskan lighting data will be very helpful, given limited WSR-88D radar coverage in Alaska as shown in Fig. ii. The full Rapid Refresh domain is shown in Fig. iv (with NLDN and Alaskan lightning data from 10 July 2007. We are very interested in accessing all possible lightning data sources within the Rapid Refresh domain for use in the Rapid Refresh 1-h data assimilation cycle.

Following figs i-iv, the remainder of the paper provides information on the RUC diabatic digital filter-based radar reflectivity algorithm (which also ingests lighting data).
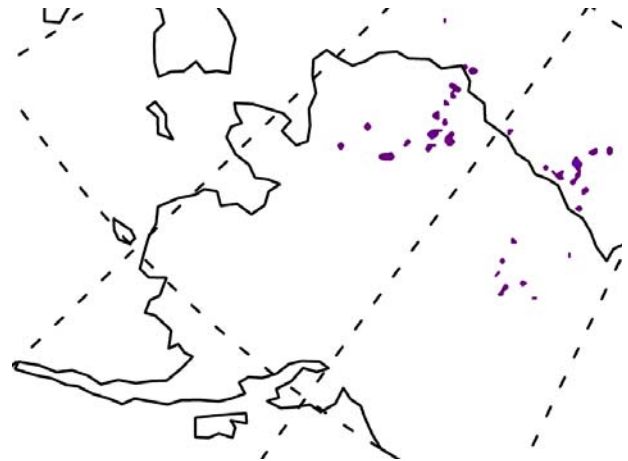


*Fig. i Lightning ground stroke density for 00z 10 July 2008 over Alaska. Information from BLM data provided by the Alaskan Region National weather Service.*
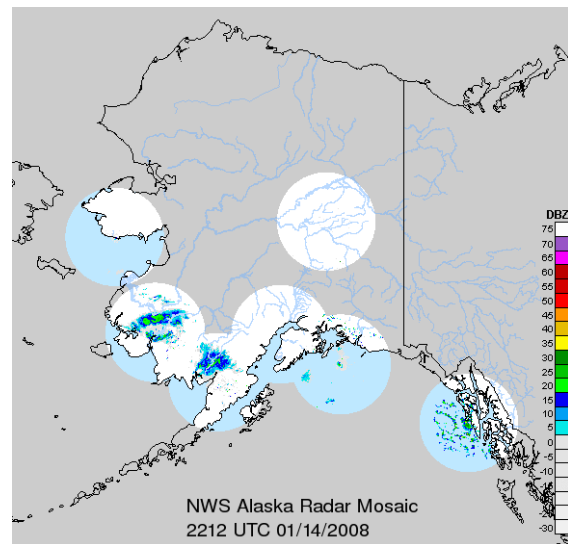


*Fig. ii Map showing low-level radar data coverage circles for the Alaskan WSR-88D radar network. Note, actual radar echoes are not time/date-matched with Fig. 10 and higher-level scans provide somewhat larger coverage*

_____

*\* Corresponding author address:* Steve Weygandt, NOAA/GSD, R/E/GSD, 325 Broadway, Boulder, CO 80305  stephen.weygandt@noaa.gov
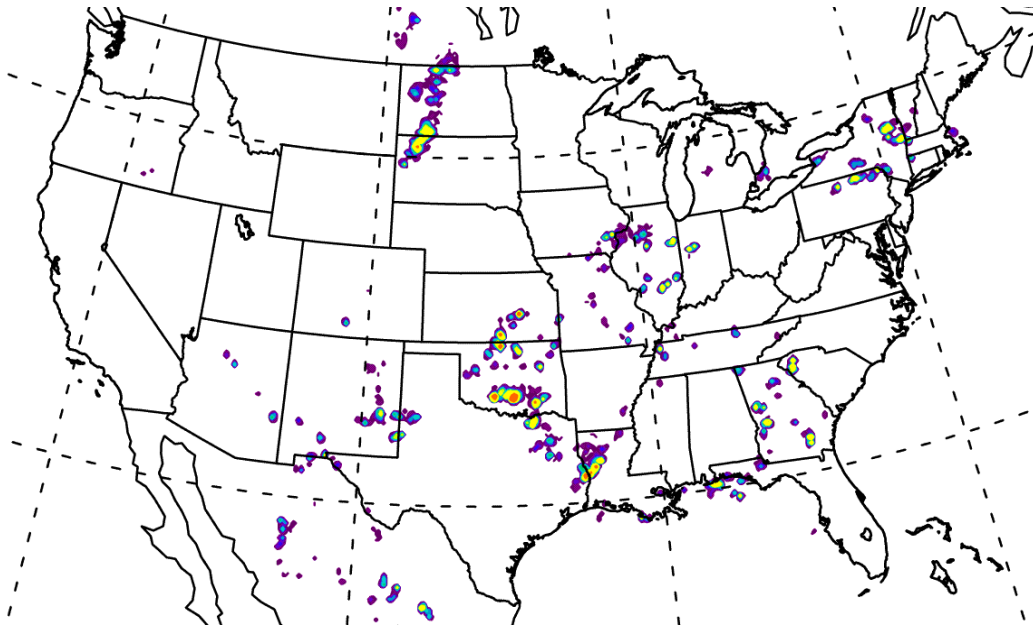
*Fig. iii  Observed lightning ground stroke density distribution over CONUS domain at 00 UTC 10 July, 2007*
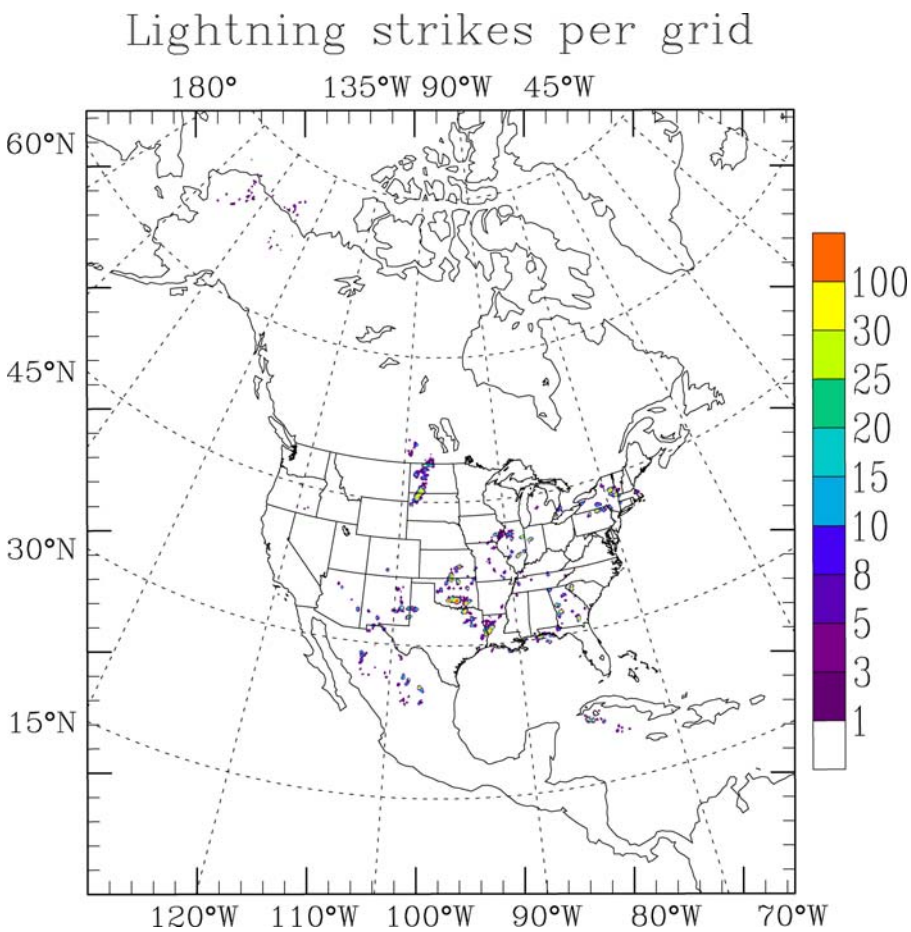


*Fig. iv  Full Rapid refresh domain with NLDN and AK BLM lightning ground stroke density data for 00z 10 July, 2007*

## 2. RUC reflectivity assimilation procedure

The Rapid Update Cycle (Benjamin et al. 2004a,c; 2006; 2007) is an hourly updated mesoscale analysis and prediction system running operationally at the National Centers for Environmental Prediction (NCEP). RUC prediction grids are used heavily as mesoscale guidance for short-range forecasts, especially by aviation, severe weather, and situational awareness forecast users. The RUC model utilizes a hybrid sigma-isentropic vertical coordinate, and includes prognostic equations for five cloud and precipitation species (following Thompson, 2004). Within the hourly RUC 3DVAR (Benjamin et al 2004c, Devenyi and Benjamin 2003) analysis, a large variety of observations are blended with the previous 1-h RUC forecast to update the mass, velocity and moisture fields. Inertial-gravity wave energy excited by the hourly assimilation is controlled by the use of a diabatic (since 2006) digital filter (Lynch and Huang 1992, Huang and Lynch 1993) within the RUC model. As depicted in Fig. 1, the digital filter includes a backward adiabatic integration followed by a weighted averaging, then a forward diabatic integration followed by a second weighted averaging to obtain a more balanced set of model initial fields.

The RUC 3DVAR analysis is complemented by a non-variational cloud analysis (Benjamin et al. 2004b, Weygandt et al. 2006a,b) in which cloud- and precipitation-related observations (METAR, satellite, radar, and lightning) are combined and used to modify the cycled cloud and precipitation fields. Hu et al. (2007) describe ongoing work to adapt the cloud analysis to the Gridpoint Statistical Interpolation (GSI) analysis package.

The new RUC radar reflectivity assimilation procedure utilizes two existing RUC system components, the cloud analysis and the diabatic digital filter initialization (DDFI), to prescribe during the pre-forecast integration a specified temperature tendency (warming) within the radar-observed reflectivity regions. This temperature tendency is deduced as a latent heating rate from the radar-observed reflectivity within the cloud analysis. Then, during the diabatic forward model integration portion of the digital filter (and within the radar reflectivity region) the model-calculated temperature tendencies from the explicit microphysics scheme and cumulus parameterization are replaced by the temperature tendency derived from the radar reflectivity data. Fig. 1 provides a schematic that illustrates the application of the latent heating based temperature



Diabatic Digital Filter Initialization (DDFI)
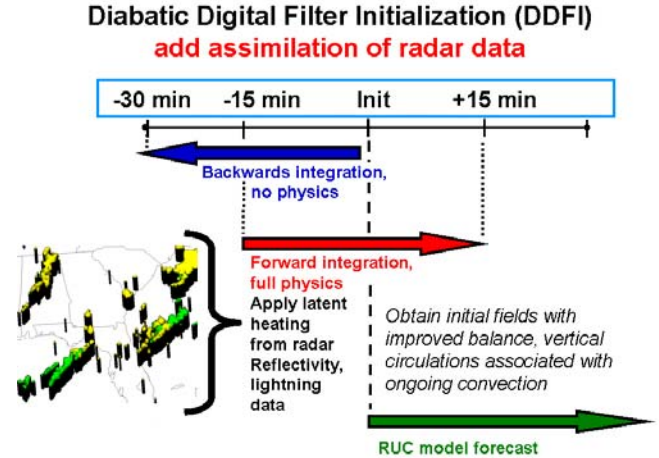add assimilation of radar data

*Fig. 1. Schematic diagram illustrating the application of the radar reflectivity-based latent heating within the diabatic digital filter initialization within the RUC model. In the sample plot, yellow and green shading show the contributions from the reflectivity and lightning data, respectively.*

tendency during the forward model portion of the DDFI. The diagnosis of the latent heating rate from the 3D radar mosaic and the NLDN data occurs within the RUC cloud analysis. First lightning ground stroke densities are used to supplement the reflectivity via a simple empirical formula. Then a latent heating rate proportional to the reflectivity intensity is found.

Information about the reflectivity and lightning data sources is as follows. The radar reflectivity used in the cloud analysis is from the NSSL national (CONUS) 3D radar mosaic grid with a 1-km horizontal resolution over 30 vertical levels and a 5-minute update cycle (Zhang et al. 2006). The data are generated by combining base level data from all available radars, performing quality control, and then combining reflectivity observations from individual radars onto a unified 3D Cartesian grid. The lightning ground stroke data is from the National Lightning Detection Network (NLDN) and can provide thunderstorm information in areas without radar coverage.

The RUC radar-enhanced DDFI method for initializing ongoing precipitation systems has a number of positive attributes. First, the method modifies the wind fields in a manner roughly consistent with the ongoing convection. Given the limitations of the observations, the horizontal grid resolution, and the parameterized representation of the convection, this is an appropriate objective. Numerous studies have shown that without modifying the wind field in this manner, the model retention of any assimilated hydrometeor information is short-lived.

Second, the modification of the wind field is done in a manner that minimizes shock to the model. Rather, the wind field evolves gradually during the DDFI to the prescribed heating rate. Note that the associated drying that would result is offset by increasing the water vapor in the reflectivity region within the cloud analysis. Third, the radar assimilation procedure requires no additional computer time, because the diabatic digital filter is already used to control noise in the RUC model initialization.

In addition to using the reflectivity data to prescribe latent heating temperature tendencies, radar reflectivity information is used to suppress model convection in areas with no echoes. In applying this convective suppression, it is extremely important to distinguish between regions with no echo and regions with no radar coverage. In these no coverage regions, the radar data cannot determine whether precipitation systems are ongoing and convective suppression is not warranted. The application of the convection suppression is as follows:
1) Determine a 2D "no echo" region, at least 100 km from any existing echo and excluding regions with no radar coverage.
2) During the DDFI and for the first 30 minutes of the model forecast, force a convective inhibition threshold condition that precludes the calling of the cumulus parameterization routine.

As a complement to the radar assimilation procedure, a suite of model simulated reflectivity fields have been added to the diagnostic fields available within the standard RUC model output grab files. The available reflectivity fields include composite, and 1-km and 4-km AGL. The fields are derived using Z-Q relationships consistent with the Thompson microphysics scheme used in the RUC and a simple power law relationship to convert the parameterized precipitation into reflectivity.

## 3. Preliminary test case results

The coding and testing of the diabatic digital filter (without the radar assimilation) was completed in early 2006 and implemented in the NCEP operational RUC in June 2006, replacing the adiabatic DFI used since 1998. The code to process the mosaic reflectivity data (interpolate the data to the RUC grid and calculate the latent heat-based temperature tendency) and apply the temperature tendency within the DDFI was completed late in 2006, and preliminary off-line testing began in January 2007. We show here results from a simple squall-line case from 00z 8 Jan 2007, in which the analysis and forecast with and without the radar

assimilation are compared. It is important to note that for this case, the radar assimilation is applied at a single analysis time, so the impact is less than can be expected when the radar assimilation is applied each hour within an evolving cycled analysis/forecast system. Because the convective suppression algorithm was added after real-time testing began, figures illustrating its impact are deferred to section 4.

Fig. 2a shows the 3-km NSSL radar reflectivity mosaic depiction of a precipitation system from 00z 8 January 2007, including a broad area of moderate radar echoes across the Mid-Atlantic States and a squall line stretching across the southeastern states. The latent heating derived from the radar reflectivity data is shown in Fig. 2b (plotted on the k= 15 RUC vertical level). The latent heating rate is plotted in deg. per 15 min with a maximum of ~ 5 K per 15 min. For this test, the heating was set proportional to the reflectivity as opposed to a reflectivity change from the background (resulting in only warming).

As expected, the application of the latent heating-based temperature tendency within the forward model integration of the DDFI (in place of the heating from the microphysical and cumulus schemes) produces a local positive temperature anomaly and induces an associated vertical circulation, with low-level convergence and upper-level divergence. Evidence of the vertical circulation can be seen in Fig. 3, which shows the difference in the west-to-east component of the wind for the experimental analysis (with the radar assimilation) relative to the control analysis (without the radar assimilation) for 2 different model levels. At low-levels (K = 15, shown Fig. 3a) the couplet of velocity differences clearly shows convergence along the squall-line. Conversely, at upper-levels (K=35, shown in Fig. 3b), a broader area of divergence is seen.

The impact of the radar data assimilation is quite evident in the resultant short-range precipitation forecast. Fig. 4 illustrates the difference between the control and radar assimilation experiment for the 1-h forecast of 15 min. accumulated total (explicit + parameterized) precipitation (45 to 60 min.). Whereas the control experiment predicts very little precipitation along the squall-line (Fig. 4a), the radar assimilation forecast produces significant precipitation along the squall line (Fig. 4b). Further examination of the precipitation fields (not shown) indicates the radar assimilation projects onto both the parameterized and grid-scale precipitation schemes within the RUC model. Forecast differences are also evident at 2 hours as shown in Fig. 5.
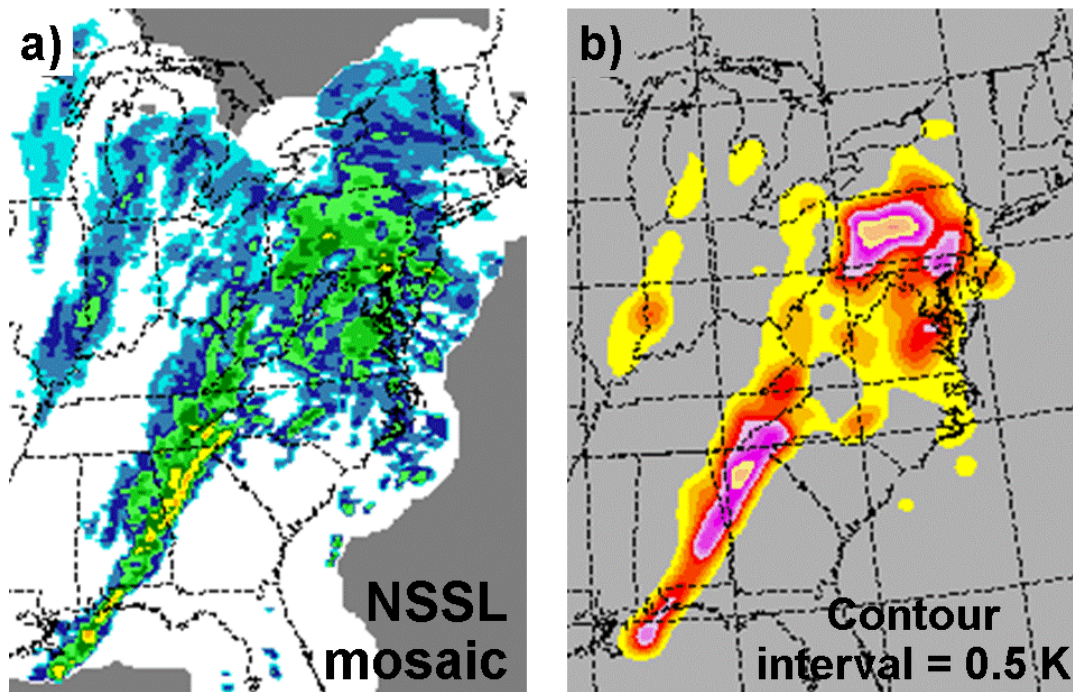
**Fig. 2. For 00z 8 January 2007. a)** *z=3-km radar reflectivity field from NSSL reflectivity mosaic (horizontally interpolated to RUC 13-km grid) plotted with a standard radar color table and **b)** radar reflectivity derived latent heat temperature tendency field for RUC model level 15 (~850 mb). Color bands are every 0.5 with a maximum of about 5.0 K / 15 min.*
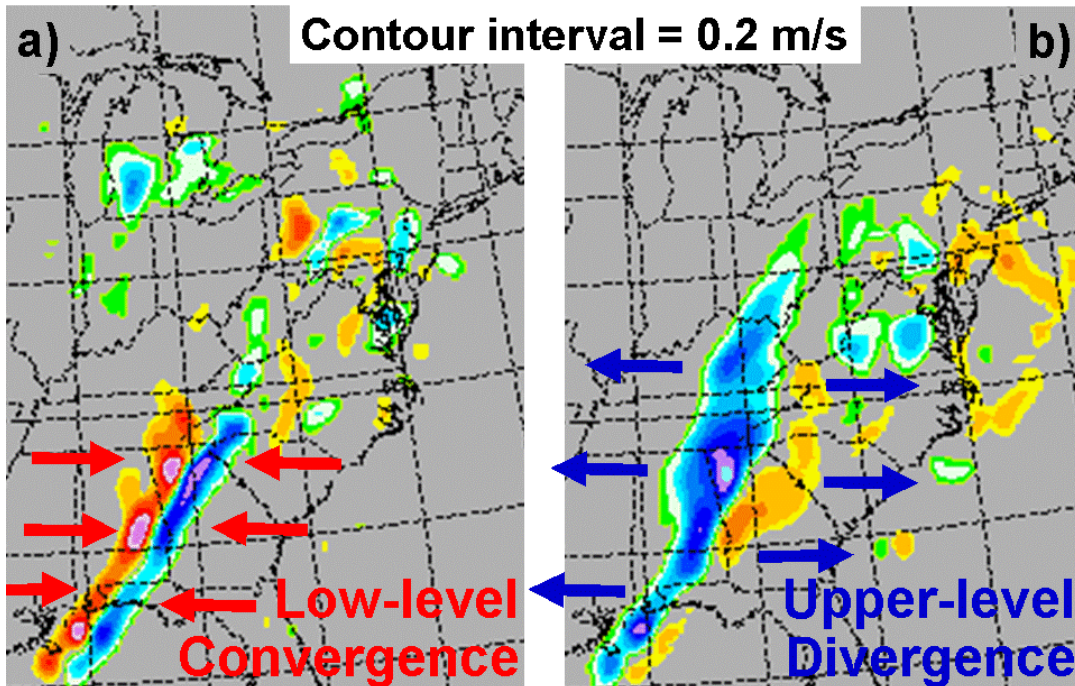


**Fig. 3. Also for 00z 8 January 2007,** *experiment differences (radar assimilation run – no radar assimilation run) in the east-west wind component for **a)** RUC model level 15 and **b)** RUC model level 35. Color bands are every 0.2 m/s with warm colors indicating enhanced westerlies in the radar assimilation experiment and cool colors indicating enhanced easterlies. As can be seen by the respective couplets, the radar assimilation induces low-level convergence and upper-level divergence along the squall-line.*
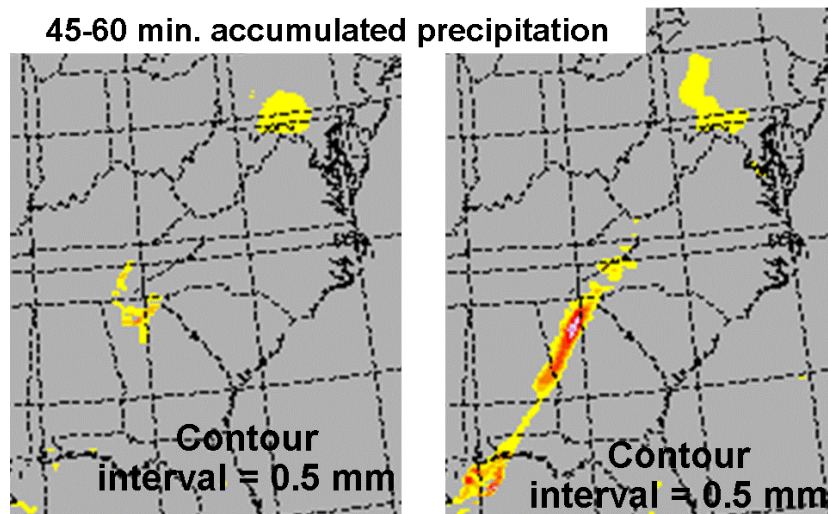
## 45-60 min. accumulated precipitation



**Fig. 4.** *1-h forecast (valid 01z 8 January 2007) of 15-min (45 to 60 min.) accumulated total precipitation (explicit + parameterized) for a) the no radar assimilation experiment and b) the radar assimilation experiment. Color bands are every 0.5 mm.*
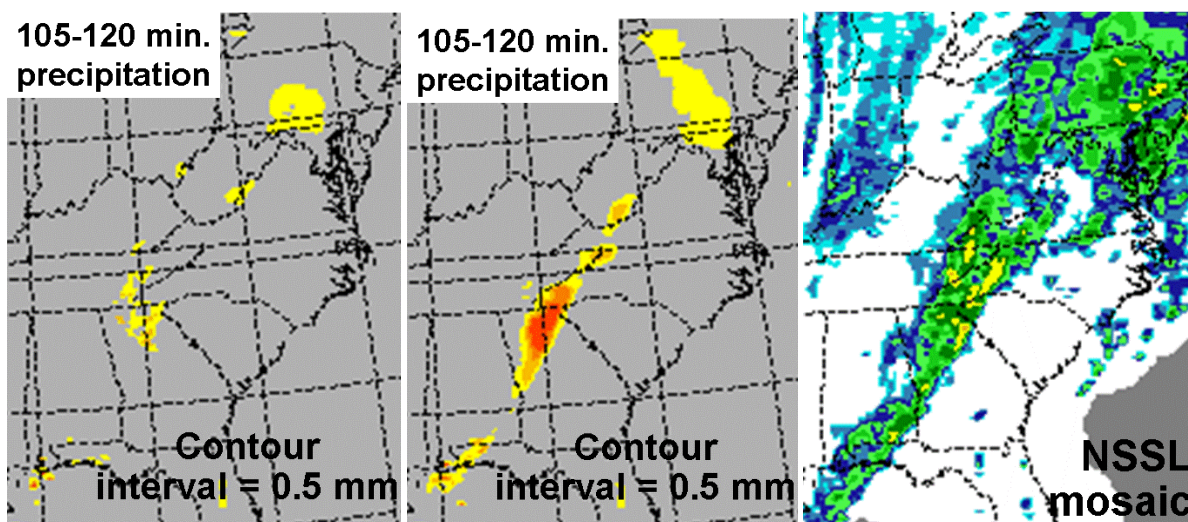


**Fig. 5.** *2-h forecast (valid 2z 8 January 2007) of 15-min (105 to 120 min.) accumulated total precipitation for a) the no radar assimilation experiment and b) the radar assimilation experiment. Color bands are every 0.5 mm. c) z= 3-km radar reflectivity from NSSL mosaic (horizontally interpolated to RUC 13-km grid) valid 02z 8 January 2007.*

Comparison of the forecast precipitation fields (Figs. 5a,b) with the radar image from 02z indicates that the model run with the radar assimilation does a better job predicting precipitation for the areas with strong radar echoes.

## 4. Real-time test cases results

Based on the encouraging results from the preliminary tests, the radar assimilation procedure was implemented in a real-time parallel RUC cycle run at GSD in February 2007. Utilizing the real-time feed of hourly radar composite data from NSSL, the radar assimilation algorithm was applied on an hourly basis. Monitoring of the real-time forecasts with the radar assimilation compared to the operational RUC forecasts without the radar assimilation has continued to reveal a short-range (3-h) positive impact in precipitation forecasts. This is clearly evident in precipitation skill-scores for a one-month comparison period shown in Fig. 6. Equitable threat scores for the radar assimilation runs remain above 0.2 for all
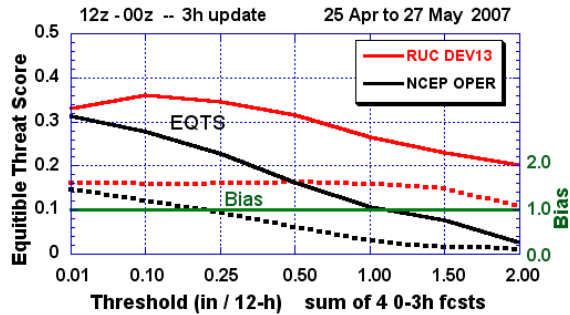
*Fig. 6. Effect of reflectivity assimilation on precipitation verification for 12-h periods from 12z to 00z (daytime) for 25 Apr – 17 May (27 cases). For each 12-h verification period, 0-3 hour forecasts from the 12, 15, 18, and 21z cycles are summed. RUC DEV13 indicates the RUC 1-h cycle with the radar assimilation; NCEP OPER indicates the NCEP operational RUC 1-h cycle without the radar assimilation.*

thresholds up to 2.0 inches. Comparable scores for the operational run (no radar assimilation) decrease dramatically to near zero for the higher thresholds. Bias scores are also more favorable for the radar assimilation run, reflecting an improvement over the operational run, which severely underpredicts the higher precipitation amounts.

Specific examples of the improvement from the radar assimilation have been easy to find in the real-time RUC forecasts. Fig. 7 shows one such case from 25 March 2007. Shown are the 3-h forecast simulated composite reflectivity for RUC runs with and without the radar assimilation. The improvement in the forecast reflectivity arc stretching from eastern Wyoming into southern Wisconsin is quite evident. The reflectivity area in northeastern Colorado also appears to be slightly better predicted in the radar assimilation run. These forecast runs were before the convective suppression algorithm was implemented and both produce considerable spurious reflectivity from Nebraska southward into Oklahoma. The impact of the convective suppression will be illustrated in a later example.

Fig. 8 illustrates another case in which the forecast impact from the radar data assimilation is readily apparent. In this wintertime situation from 12 February 2007, the radar data assimilation helps in three distinctly different precipitation regimes: 1) a band of stable ascent snow extending from southern Wisconsin to northern Indiana, 2) an arc of rain and showers stretching from northwest Texas across Oklahoma and 3) a mesoscale area of convective showers across the Florida Peninsula. Comparison of Figs. 8a and 8b clearly shows the
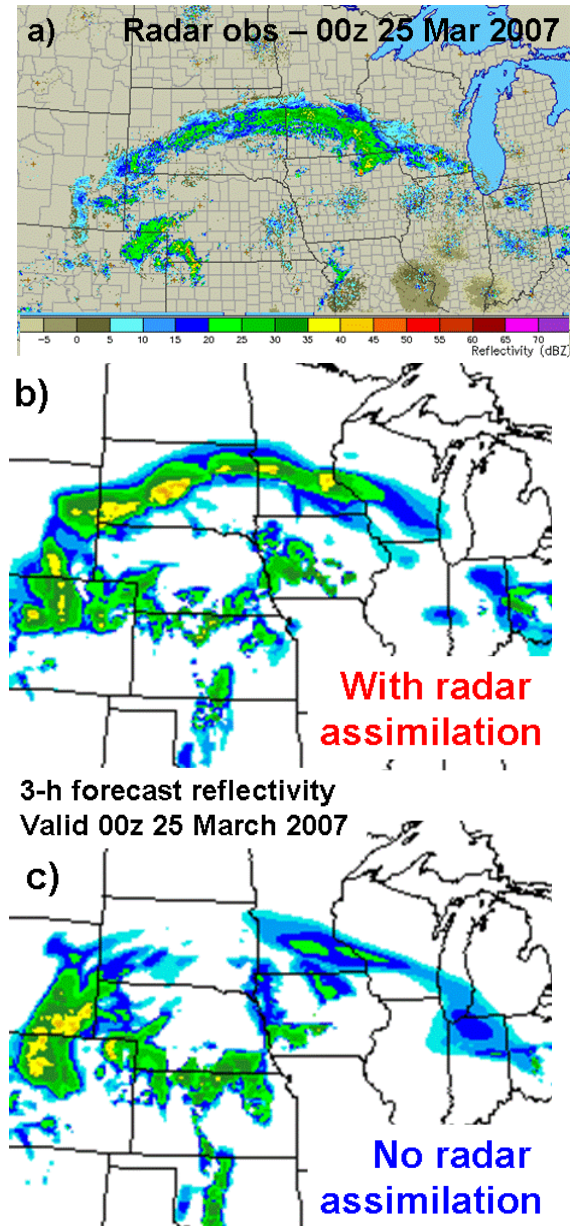


*Fig. 7. Sample improvement from radar assimilation as reflected in the new RUC simulated reflectivity field for 3-h forecast valid 00z 25 March 2007. a) observed radar reflectivity, b) RUC forecast with radar assimilation, and c) RUC forecast without radar assimilation.*

enhancement of the upward motion in the initial vertical velocity field in each of the three areas. It is important to remember that this enhanced upward motion and the associated low-level convergence / upper level divergence couplets (not shown) develop in response to the heating that is prescribed
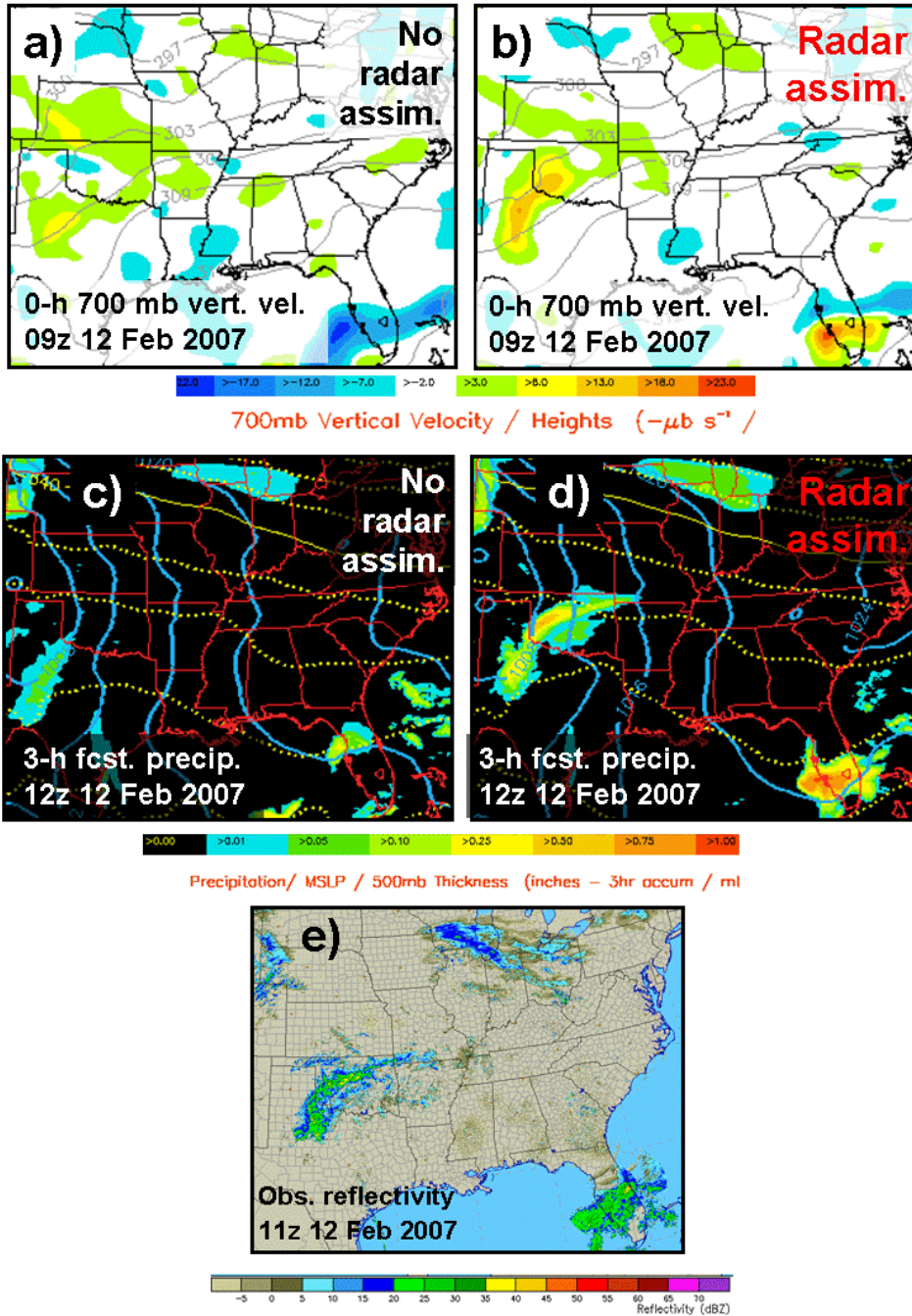
**Fig. 8. Improvement from radar assimilation for RUC forecasts initialized 09z 12 February 2007. Shown are RUC initial 700 hPa vertical velocity fields (after the diabatic digital filter initialization) for a) radar assimilation run and b) no radar assimilation run, followed by 3-h RUC forecast precipitation fields (valid 12z 12 February 2007) for c) radar assimilation run and d) no radar assimilation run. e) shows 11z 12 February 2007 observed radar reflectivity.**

during the diabatic forward integration portion of the digital filter initialization. Because the digital filter is utilized to minimize spurious inertial-gravity wave energy in the early part of the forecast, the vertical circulations induced by the radar assimilation are produced with a minimum of shock to the model. Comparison of the resultant

3-h precipitation forecasts (Figs. 8c,d) with the 11z radar echoes shows a better qualitative agreement for the radar assimilation experiment.

The next case, shown in Fig. 9, depicts a more intense convective event from 1 March 2007, again before the convective suppression algorithm was
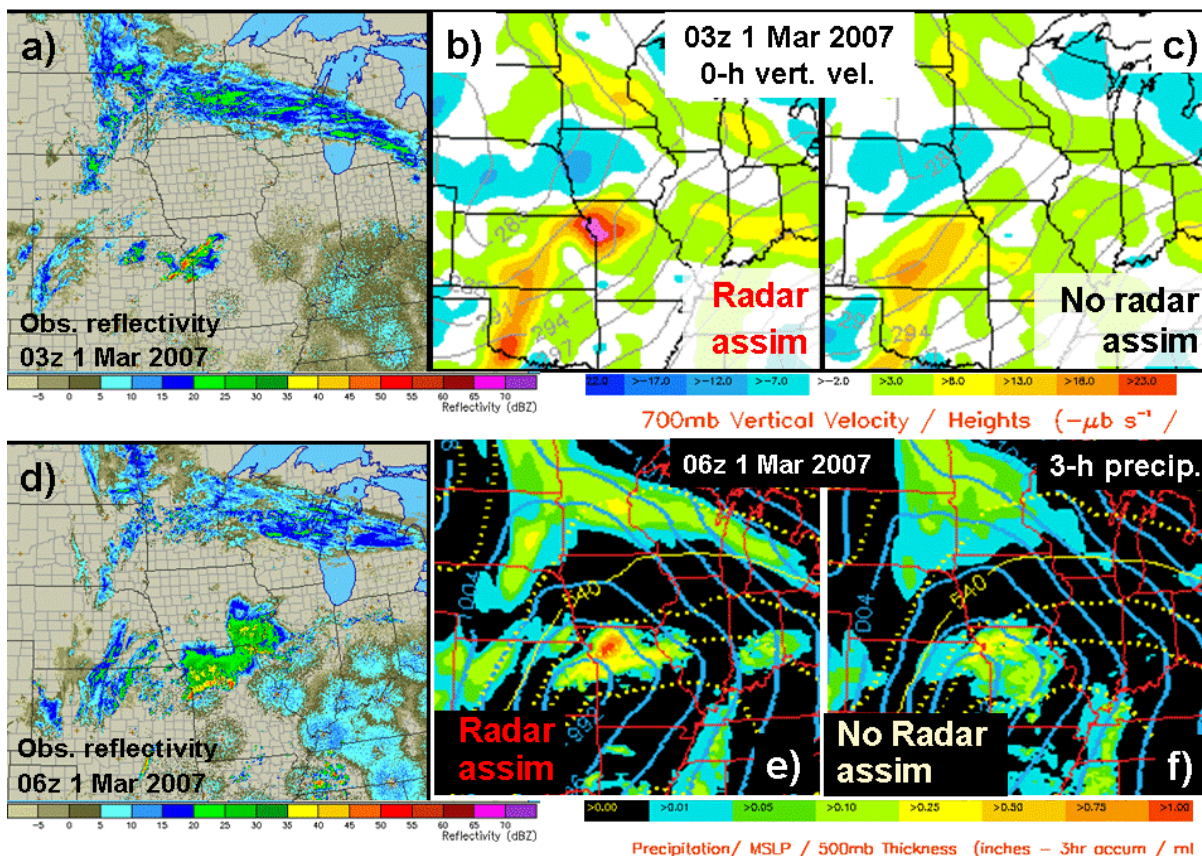
*Fig. 9. Improvement from radar assimilation for RUC forecasts initialized 03z 1 March 2007. Shown are RUC initial 700 mb vertical velocity fields (after the diabatic digital filter initialization) for b) radar assimilation run and c) no radar assimilation run, followed by 3-h RUC forecast precipitation fields (valid 06z 1 March 2007) for e) radar assimilation run and f) no radar assimilation run. a) and d) show 03z and 06z 1 March 2007 observed radar reflectivity, respectively.*

implemented. At the model initial time, 03z, a cluster of intense thunderstorms was ongoing just to the south of Kansas City (Fig. 9a). Comparison of Figs. 9b and 9c illustrates the ability of the radar assimilation algorithm to introduce a strong mesoscale vertical velocity maximum and associated low-level convergence / upper-level divergence (not shown) signal in the region of intense convection. In the absence of the radar assimilation, a weaker, broader-scale vertical velocity maximum is shown to the southwest where no radar echoes are shown. Comparison of the resultant 3-h precipitation fields (Fig. 9e,f) shows that the radar assimilation forecast produces much larger precipitation amounts around the area of intense convection. In contrast, the run without the radar assimilation produced only a broad area of light precipitation across Missouri.

The radar reflectivity field from 3z shows that the cluster of storms has evolved into a mesoscale precipitation area with a leading edge of strong storms. In addition there has been northeastward

development of radar echoes into southeastern Iowa. While the comparison of 3-h precipitation with an instantaneous radar reflectivity field is problematic, the radar assimilation forecast appears qualitatively to be a better forecast.

A final example to illustrate the impact from the convective suppression algorithm is now presented. Fig. 10a shows the NSSL radar reflectivity field from 12z 7 June 2007. Outside the radar echo regions, black indicates no echo and grey indicates no radar coverage. Fig. 10b is the corresponding radar suppression template. Yellow areas are obtained by extending outward ~ 100 km from ongoing regions of convection and signify regions where convection will not be suppressed. Cyan areas indicate regions outside the radar coverage where convection will also not be suppressed. Grey areas are regions where convection will be suppressed during the first 30 minutes of the model integration and require at least a 300 hPa deep convection free layer. The radar-defined regions of convective suppression
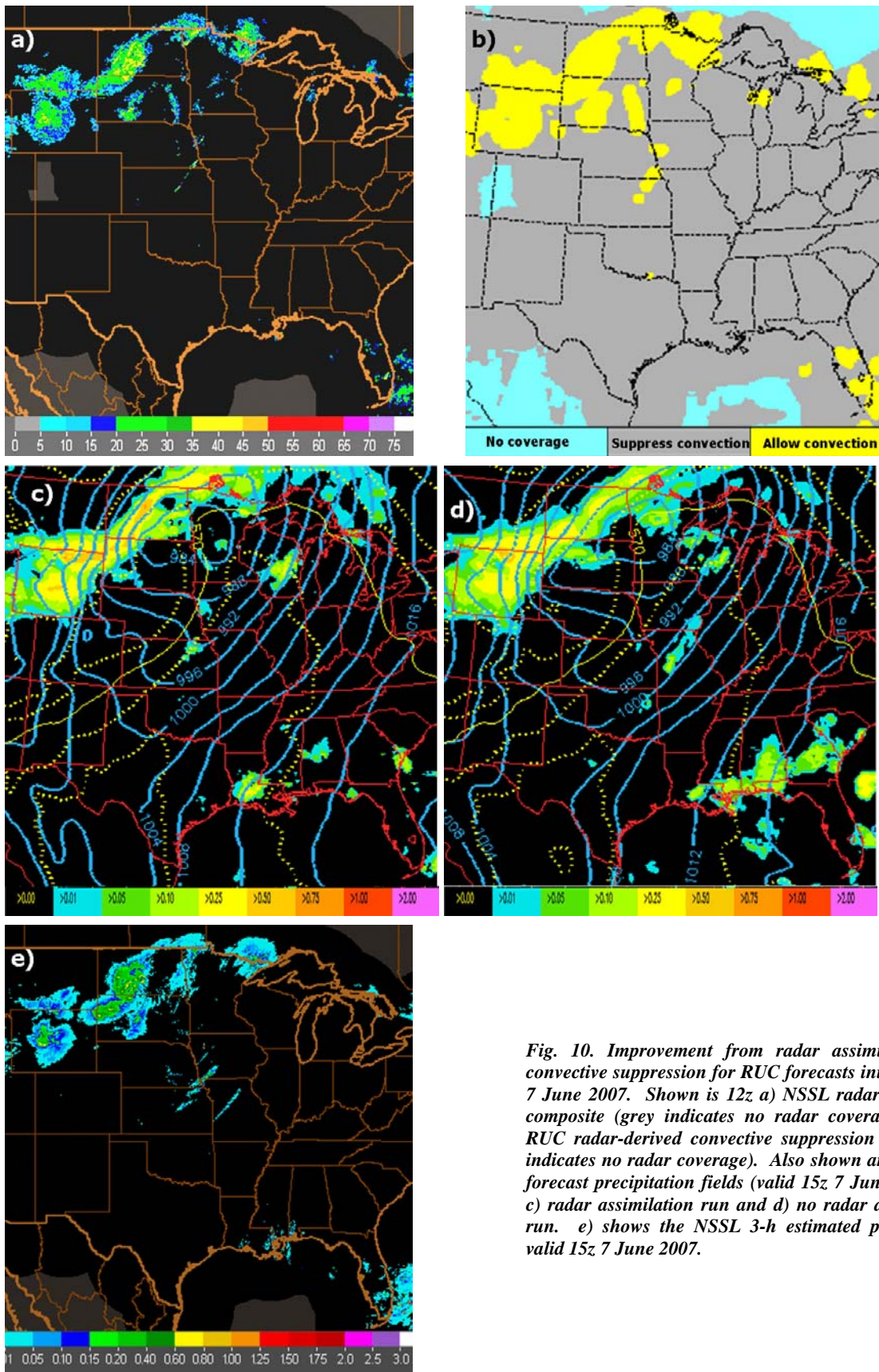
Fig. 10. Improvement from radar assimilation and convective suppression for RUC forecasts initialized 12z 7 June 2007. Shown is 12z a) NSSL radar reflectivity composite (grey indicates no radar coverage) and b) RUC radar-derived convective suppression map (cyan indicates no radar coverage). Also shown are 3-h RUC forecast precipitation fields (valid 15z 7 June 2007) for c) radar assimilation run and d) no radar assimilation run. e) shows the NSSL 3-h estimated precipitation valid 15z 7 June 2007.

are augmented by regions where the GOES cloud top pressure data indicate the entire column is clear. This explains regions of convective suppression over Mexico and the Gulf of Mexico in Fig 10b, which are indicated in Fig. 10a to have no radar data coverage. This merging of cloud and precipitation observation information, where appropriate, to provide a more coherent picture of cloud and precipitation processes is consistent with the principles of the RUC and ARPS cloud analysis schemes. These schemes are being combined to create a more general cloud analysis scheme as summarized by Hu et al. (2007).

One additional note about the convective suppression concerns the radar coverage in the west. Because of the greater radar spacing (compared to the more populated east) and to a lesser extent the greater prevalence of beam blockage (due to the more mountainous terrain), the lower portions of the atmosphere have very poor coverage for certain regions of the west. This was clearly evident, when we initially required a 500 hPa (subsequently modified to 300 hPa) deep echo-free layer for suppressing convection and found that for large areas of Nevada and Utah and a small area of northeastern Wyoming and southeastern Montana, convective suppression was not possible. Moreover, it is important to remember that the radar characterization of precipitation systems in these areas is significantly impacted due to the extensive area with no low-level radar coverage.

Figs.10c,d show the resultant 3-h precipitation forecast from a parallel RUC run with the radar assimilation (and convective suppression algorithm) and the operational RUC run (with neither algorithm). For comparison, the NSSL estimated 3-h accumulated precipitation (valid 15z) is shown in Fig. 10e. The principal difference between the two RUC forecasts is across the southeastern states, for which the spurious precipitation is greatly reduced in the run with the convective suppression. Other differences are more subtle, consistent with the strongly forced nature of the weather pattern on this day. It does appear, however, that the radar assimilation run does a better job of limiting precipitation across northeastern North Dakota and northcentral Minnesota. Although the precipitation across northeastern Wyoming appears overdone in both model forecasts, as noted above this area has very poor low-level radar coverage.

## 5. Summary and outlook

As detailed in Benjamin et al. (2007), code has been transferred to NCEP for a bundle of RUC upgrades, including the radar assimilation and convective suppression packages. Real-time and retrospective runs at NCEP are underway in anticipation of a likely RUC upgrade later this year. Related work at NCEP to make the reflectivity mosaic available in real-time was completed in the fall of 2007 and the national reflectivity mosaic data are being used in the parallel runs at NCEP. Monitoring of real-time parallel cycles at GSD and NCEP continues.

In anticipation of inclusion of a similar radar assimilation algorithm in the Rapid Refresh (RR), additional work has been completed to develop a diabatic digital filter initialization procedure within the WRF core selected for the Rapid Refresh. As with the RUC, the WRF-based RR model will be cycled hourly with new analyses supplied by a specially adapted GSI (Devenyi et al. 2007). Work has also been completed to incorporate a generalized cloud analysis (including radar assimilation) into the GSI analysis procedure (Hu et al. 2008), from which latent heating fields can be derived for use within the RR digital filter initialization.

Additional possible work will examine the utility of hourly initializing 3-km explicit convection resolving forecasts (over a limited northeastern U.S. domain) from 13-km RUC fields following the application of the radar assimilation-based diabatic digital filter initialization.

## 6. Acknowledgments

# 7. References

Benjamin, S., D. Devenyi, T. Smirnova, S. Weygandt, J. M. Brown, S. Peckham, K. Brundage, T. L. Smith, G. Grell, and T. Schlatter, 2006: From the 13km RUC to the Rapid Refresh. *12th Conference on Aviation Range and Aerospace Meteorology*, Atlanta, GA, American Meteorological Society, 9.1.

Benjamin, S., and co-authors, 2007: From the radar enhanced RUC to the WRF-based Rapid Refresh. *18$^{th}$ Conf. Num. Wea. Pred.,* Park City, UT, AMS, J3.4.

Benjamin, S. G., G. A. Grell, J. M. Brown, T. G. Smirnova, and R. Bleck, 2004a: Mesoscale Weather Prediction with the RUC Hybrid Isentropic/Terrain-Following Coordinate Model. *Monthly Weather Review*, **132,** 473-494.

Benjamin, S. G., S. S. Weygandt, J. M. Brown, T. L. Smith, T. Smirnova, W. R. Moninger, and B. Schwartz, 2004b: Assimilation of METAR cloud and visibility observations in the RUC. *11th Conference on Aviation, Range, Aerospace and 22nd Conference on Severe Local Storms*, Hyannis, MA, American Meteorology Society, 9.13.

Benjamin, S. G., D. Devenyi, S. S. Weygandt, K. J. Brundage, J. M. Brown, G. A. Grell, D. Kim, B. E. Schwartz, T. G. Smirnova, T. L. Smith, and G. S. Manikin, 2004c: An Hourly Assimilation/Forecast Cycle: The RUC. *Monthly Weather Review*, **132,** 495-518.

Devenyi, D. and S. Benjamin, 2003: A variational assimilation technique in a hybrid isentropic-sigma coordinate. *Meteor. Atmos. Phys.,* **82,** 245-257.

Devenyi, D., S. Weygandt, T. Schlatter S. Benjamin, and M. Hu, 2007: Hourly data assimilation with the Gridpoint Statistical Interpolation for Rapid Refresh. *18$^{th}$ Conf. Num. Wea. Pred.,* Park City, UT, AMS, 4A.2.

Hu, M., S. Weygandt, M. Xue, and S. Benjamin, 2007: Development and testing of a cloud analysis package using radar, satellite, and surface cloud observations within GSI for initializing Rapis Refresh. *18$^{th}$ Conf. Num. Wea. Pred.,* Park City, UT, AMS, P2.5.

Huang, X. and P. Lynch, 1993: Diabatic digital-filtering initialization: Application to the HIRLAM model. *Monthly Weather Review*, **121,** 589-603.

Lynch. P. and X. Huang, 1992: Initialization of the HIRLAM model using a digital filter. *Monthly Weather Review*, **120,** 1019-1034.

Thompson, G., R. M. Rasmussen, and K. Manning, 2004: Explicit Forecasts of Winter Precipitation Using an Improved Bulk Microphysics Scheme. Part I: Description and Sensitivity Analysis. *Monthly Weather Review*, **132,** 519-542.

Weygandt, S., S. G. Benjamin, D. Dévényi, J. M. Brown, and P. Minnis, 2006a: Cloud and hydrometeor analysis using metar, radar, and satellite data within the RUC/Rapid-Refresh model. *12th Conference on Aviation Range and Aerospace Meteorology*, Atlanta, GA.

Weygandt, S.S., S.G. Benjamin, J.M. Brown, and S.E. Koch, 2006b: Assimilation of lightning data into RUC model forecasting. *2nd Intl. Lightning Meteorology Conf.* Tucson, AZ

Zhang, J., C. Langston, K. Howard, and B. Clarke, 2006: Gap-filling in 3D radar mosaic analysis using vertical profiles of reflectivity. *12th Conference on Aviation Range and Aerospace Meteorology*, Atlanta, GA.